aggregation and liquid-crystalline ordering in these systems, which leads to an anomalous behavior.[24] Efforts are underway to adapt the representation of $\sigma_{flexible}$ used in this work (cf. eq 9 and 14) and Lee's description of excluded volume to the highly disperse particle populations characteristic of solutions of reversibly polymerizing proteins[23,25,26] or surfactant micelles.[27,28]

Acknowledgment. I thank Prof. Judith Herzfeld, Mark Taylor, and Xin Wen for a critical reading of the manuscript and, in particlar, Prof. Herzfeld for a number of useful suggestions. This work was supported by NIH Grant HL 36546 and the Deutsche Forschungsgemeinschaft.

References and Notes

(1) Straley, J. P. *Mol. Cryst. Liq. Cryst.* **1973**, *22*, 333.
(2) Odijk, T. *Macromolecules* **1986**, *19*, 2313.
(3) Grosberg, A. Yu.; Khokhlov, A. R. *Soc. Sci. Rev. A Phys.* **1987**, *8*, 147.
(4) Itou, T.; Teramoto, A. *Macromolecules* **1988**, *21*, 2225.
(5) Khokhlov, A. R.; Semenov, A. N. *Physica* **1981**, *108A*, 546; **1982**, *112A*, 605.
(6) Lee, S. *J. Chem. Phys.* **1987**, *87*, 4972.
(7) Kubo, K.; Ogino, K. *Mol. Cryst. Liq. Cryst.* **1979**, *53*, 207.
(8) Kubo, K. *Mol. Cryst. Liq. Cryst.* **1981**, *74*, 71.
(9) Onsager, L. *Ann. N.Y. Acad. Sci.* **1949**, *51*, 627.
(10) Alben, R. *Mol. Cryst. Liq. Cryst.* **1971**, *13*, 193.
(11) Lasher, G. *J. Chem. Phys.* **1970**, *53*, 4141.
(12) Cotter, M. A. *J. Chem. Phys.* **1977**, *66*, 1098.
(13) Parsons, J. D. *Phys. Rev. A* **1979**, *19*, 1225.
(14) Boublík, T.; Nezbeda, I. *Collect. Czech. Chem. Commun.* **1986**, *51*, 2301.
(15) Frenkel, D. *J. Phys. Chem.* **1987**, *91*, 4912.
(16) Stroobants, A.; Lekkerkerker, H. N. W.; Frenkel, D. *Phys. Rev. A* **1987**, *36*, 2929.
(17) Poniewierski, A.; Holyst, R. *Phys. Rev. Lett.* **1988**, *61*, 2461.
(18) Somoza, A. M.; Tarazona, P. *Phys. Rev. Lett.* **1988**, *61*, 2566.
(19) Khokhlov, A. R.; Semenov, A. N. *J. Stat. Phys.* **1985**, *38*, 161.
(20) Lifshitz, I. M. *Sov. Phys.—JETP (Engl. Transl.)* **1969**, *28*, 1280.
(21) Schmidt, M. *Macromolecules* **1984**, *17*, 553.
(22) Parthasarathy, R.; Houpt, D. J.; DuPré, D. B. *Liq. Cryst.* **1988**, *3*, 1073.
(23) Herzfeld, J.; Taylor, M. P. *J. Chem. Phys.* **1988**, *88*, 2780.
(24) Odijk, T. *J. Phys. (Les Ulis, Fr.)* **1987**, *48*, 125.
(25) Hentschke, R.; Herzfeld, J. *J. Chem. Phys.* **1989**, *90*, 5094.
(26) Herzfeld, J.; Briehl, R. W. *Macromolecules* **1981**, *14*, 1209.
(27) McMullen, W. E.; Gelbart, W. M.; Ben-Shaul, A. *J. Chem. Phys.* **1985**, *82*, 5616.
(28) Taylor, M. P.; Berger, A.; Herzfeld, J. *J. Chem. Phys.* **1989**, *91*, 528.

Registry No. γ-Benzyl-L-glutamate (SRU), 25038-53-3; γ-benzyl-L-glutamate (homopolymer), 25014-27-1.

Kinetics of Mesophase Transitions in Thermotropic Copolyesters. 3. Poly[(phenyl-*p*-phenylene terephthalate)-*co*-[(1-phenylethyl)-*p*-phenylene terephthalate]] Copolyester

Stephen Z. D. Cheng,* Anqiu Zhang,† Ronald L. Johnson, and Zongquan Wu†

Institute and Department of Polymer Science, College of Polymer Science and Polymer Engineering, The University of Akron, Akron, Ohio 44325-3909

Hak Hung Wu

Granmont Inc., 2790 Columbus Road, Granville, Ohio 43023. *Received June 13, 1989; Revised Manuscript Received August 28, 1989*

ABSTRACT: Structure formation kinetics of a copolyester consisting of *p*-benzenedicarboxylic acid (TPA), phenylhydroquinone (PHQ), and (1-phenylethyl)hydroquinone (PEHQ) with a molar ratio of 50/25/25 has been studied. This copolyester shows periodic *c*-axis order in its X-ray diffraction pattern due to equal unit lengths of the comonomers. The crystal unit cells for quenched and annealed TPA/PHQ/PEHQ copolyester are both monoclinic but with slightly different sizes. Two transition processes from its nematic to solid states can also be identified. Isothermal kinetics of the transitions indicate that the fast transition process is nucleation-controlled crystal growth. The development of the slow process is hampered by the previously grown crystals in the fast process. A higher transition temperature of the fast transition process compared with that of the slow process is attributed to a larger enthalpy change (thermodynamic effect) and melting of relatively ordered domains (kinetic effect) during this transition.

Introduction

During the last 10 years, there has been an increasing interest in the development of thermotropic liquid crystalline polyesters in both academic and industrial areas of research. From the engineering point of view, a lowering of transition temperatures of the polyesters due to the limitation of processing conditions is desirable, as well as enhancement of the anisotropic nature of their flow behavior (low viscosity above their transition temperatures) and their ultimate mechanical properties. One way to approach such goals is to copolymerize different aromatic ester monomers to disturb the regularities of the polyester crystalline structures. Basically, two different paths can be carried out. The first is the path of disturbing the regularities along the chain axis by introducing different monomer lengths, such as in the case of the Xydar copolyesters consisting of *p*-dihydroxybenzoic acid (HBA), 4,4′-dihydroxybiphenyl (HBP), and *p*-benzenedicarboxylic acid (TPA), or introducing additional solid kinks, such as in the case of the Vectra copolyesters with HBA and 6-hydroxy-2-naphthoic acid (HNA). From crystalline structural characterization by wide-an-

† On leave from China Textile University, Shanghai, China.

0024-9297/90/2223-1196$02.50/0

gle X-ray diffraction (WAXD) experiments, aperiodic c-axes can be observed. The second is the path of disturbing the regularities of the lateral packings by introducing pendant side groups, such as in the case of a poly[(phenyl-p-phenylene terephthalate)-co-[(1-phenylethyl)-p-phenylene terephthalate]] copolyesters consisting of TPA, phenylhydroquinone (PHQ), and (1-phenylethyl)hydroquinone (PEHQ) (TPA/PHQ/PEHQ, 50/25/25). The WAXD pattern indicates that this copolyester shows periodic c-axis order since it contains the comonomers in equal lengths.

It is now well-known that for the copolyesters of HBA/HNA and HBA/HBP/TPA types two transition processes exist during the transitions from their nematic to solid states.[1] A fast transition process occurs via aggregation of the chain molecules within a very short time period (usually, a few seconds) during quenching, and a slow transition process develops gradually during the latter annealing.[1] X-ray diffraction patterns indicate that in both copolyesters a hexagonal packing with a cylindrical symmetry along the chain direction forms in the fast process, and an orthorhombic packing develops in the slow transition process.[2-4] Blackwell et al.[3,5-7] have developed an analytical method to determine the randomness of the distribution of the comonomer units in these copolyesters on the basis of their WAXD pattern along the aperiodic meridional directions. Nevertheless, the origin of these two transition processes in these copolyesters is still a debatable topic, and we are still some distance from a proper understanding of the phenomenon.

We have asked ourselves whether for the TPA/PHQ/PEHQ types of copolyesters the same phenomena can still be observed. It should be noted, again, that they have large pendant side groups. On the other hand, all three comonomers have the same unit lengths of about 6.4 Å. In this paper, we report our recent crystalline structural and transition kinetic studies on this copolyester. From our experimental observations two monoclinic crystal packings can be observed in this copolyester, which are assigned to be monoclinic I and monoclinic II. The monoclinic I form corresponds to the as-spun fiber (quenched) and the monoclinic II form to the annealed fiber. These two packings have slightly different crystal unit cell sizes as well as angles of γ. Two transition processes can still be identified: a fast process and a slow process in the TPA/PHQ/PEHQ samples although this fast transition process is structurally different from those in the cases of Vectra and Xydar copolyesters. The kinetics of the fast transition process in this copolyester can be traced as well as the relationship between these two transition processes. We also attempt to explain why the fast transition process shows a higher transition temperature.

Experimental Section

Materials and Samples. The copolyester TPA/PHQ/PEHQ (50/25/25) was kindly provided by Granmont Inc. of Granville, OH. The statistical molar mass of the repeating units is 165.16 g/mol. On the basis of the information obtained, the copolyester was synthesized via a direct condensation reaction of the three monomers in their solution states. To increase the molecular mass, solid-state polymerization was carried out after precipitation and drying of the copolyester at 573 K for 24 h.

In order to study the crystal unit cells in the copolyester, melt-spun fibers from its nematic phase (635 K) were examined in our laboratory. The diameter of a single fiber was about 1 denier. The drawn ratio of the fiber is about 50×. The fibers were examined in the as-spun state and after annealing at 590 K for 4 h under load. Specimens for X-ray analysis were prepared as parallel bundles of ~50 fibers.

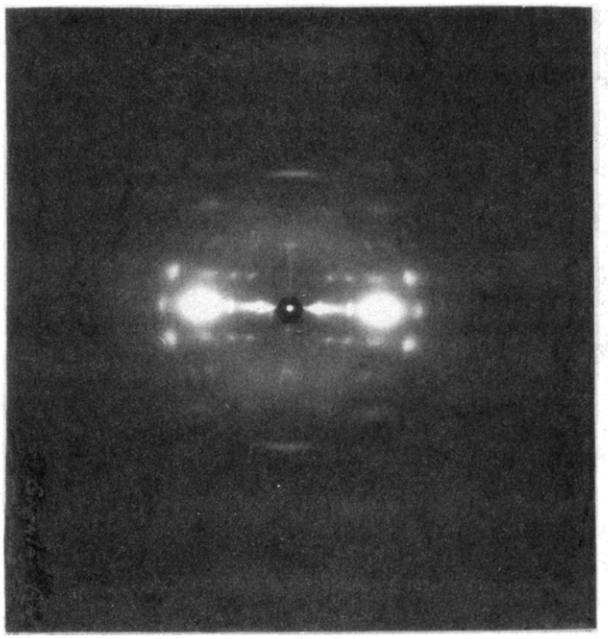

Figure 1. Wide-angle X-ray diffraction photograph of the TPA/PHQ/PEHQ copolyester fibers annealed at 590 K for 4 h under load (medium exposure time).

Both fiber and bulk samples were prepared then put into DSC pans. The sample weights were controlled in a range of 15–20 mg. All pan weights were within a deviation of ±0.002 mg.

Wide-Angle X-ray Diffraction (WAXD). X-ray experiments were carried out on a Rigaku X-ray generator with a 12-kW rotating anode as a source of the incident X-ray beam. The point-focused beam is monochromatized with a graphite crystal and a pulse-height analyzer sensitive to Cu Kα radiation. X-ray fiber diagrams were recorded on a vacuum camera. The d spacings were calibrated with silicon powder (325 mesh size).

Differential Scanning Calorimetry (DSC). In order to study the transition behavior of the copolyesters, DSC measurements were carried out on both a Du Pont 9900 thermal analyzer and a Perkin-Elmer DSC2. The DSCs were carefully calibrated for temperature, heat flow, and heat capacity following the standard procedures we apply in our laboratory.[1] The fiber samples were heated from room temperature to 640 K at a 10 K/min heating rate. The heating traces were recorded. The bulk samples were used to study isothermal transition kinetics. They were heated to 640 K and held for 1.5 min. Then the samples were quickly cooled to the predetermined crystallization temperature, T_c, and kept there for different fixed time periods, t_c. The samples were reheated to 640 K at a 10 K/min heating rate.

In this paper, peak temperatures were used as T_d. When two transition peaks were observed during heating, their temperatures were distinguished to be T_d(h) for the high-temperature peak and T_d(l) for the low-temperature peak. In order to avoid any influence of previous thermal history, every sample was used only once.

Results and Analyses

Determinations of Crystal Unit Cells. Figure 1 shows a typical fiber diagram of the crystal diffraction photograph for the annealed TPA/PHQ/PEHQ copolyester. Along the equator, there are seven diffraction spots that can be identified. Additionally, a short-time exposed photograph was used to help identify the very strong diffraction spots shown in Figure 2. Along the meridian, periodic diffraction spots can be clearly observed for up to six layers. The even numbered layers show strong diffraction spots, and the odd numbered layers are missing or barely seen, indicating a $p2_1$ space group. On the quadrants, five spots along the first, second, and the third

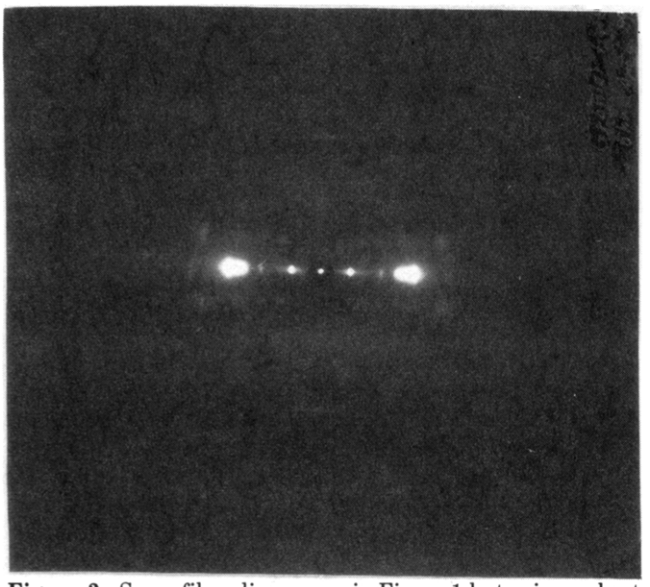

Figure 2. Same fiber diagram as in Figure 1 but using a short exposure time.

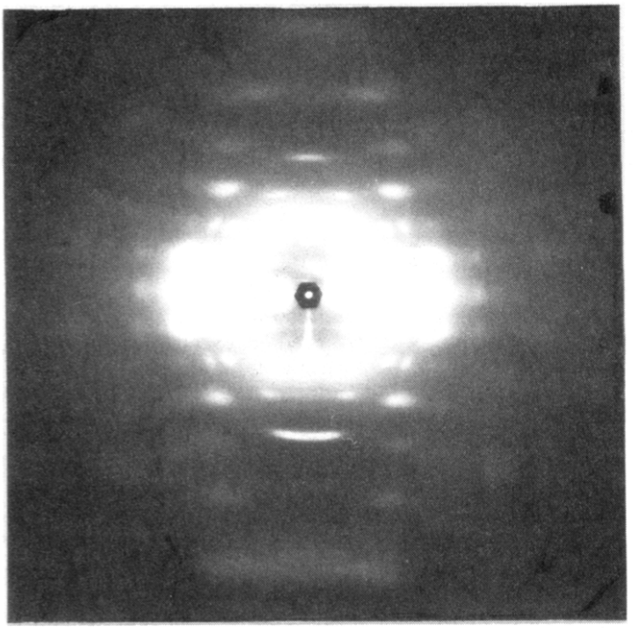

Figure 3. Same fiber diagram as in Figure 1 but using a prolonged exposure time.

layers, three along the fourth layer, and one along the fifth layer can be seen. In order to observe the weak diffraction spots, a prolonged time exposed photograph was taken as shown in Figure 3. A detailed listing of the 26 experimental 2θ angles, d spacings, and the corresponding intensities of the diffraction spots are listed in Table I.

To determine the size and shape of the crystal unit cell for our fiber diagrams as shown in Figures 1–3, we ordinarily begin by trying to find an $hk0$ reciprocal lattice net, namely, a parallelogram with edges a^* by b^* that accounts for the values determined from the equatorial diffractions. The smallest distance between the center of the X-ray incident beam and the diffraction spot corresponds to a low index. From Figures 1–3, one can find that there is a missing spot on the equator, which can be found on the first layer of quadrants. With this diffraction spot assigned as 011 to form a $hk0$ reciprocal lattice net, all other diffraction spots shown in Figures 1–3 can be fitted into this net. The l index of each diffraction can also be determined by the layer line on which the diffraction lies and the c crystallographic axis is readily determined from the layer line spacing. After least-square refinements via computer, we found that the crystal unit cell of annealed TPA/PHQ/PEHQ copolyester is monoclinic II with a = 13.30 (±0.01) Å, b = 9.693 (±0.01) Å, c = 12.51 (±0.01) Å, and γ = 76.1° (±0.1°). This leads to a volume of 1565.1 Å^3. In each unit cell four chains are contained. The calculated crystallographic density is thus 1.402 g/cm^3. The experimental density is 1.359 g/cm^3, determined by density gradient measurements. All the calculated and experimentally observed d spacings for each hkl crystal plane have also been listed in Table I for comparison.

Table I
Experimental and Calculated Crystallographic Parameters of the Monoclinic II Crystal Unit Cell for Annealed TPA/PHQ/PEHQ Copolyester Fibers[a]

	2θ, deg		d spacing, Å		
(hkl)	exptl	calcd	exptl	calcd	intensity[b]
(100)	6.879	6.847	12.85	12.91	vs
(200)	13.85	13.72	6.392	6.453	s
($\bar{2}$10)	18.32	18.44	4.919	4.810	s
(020)	18.60	18.86	4.770	4.705	s
(300)	20.94	20.65	4.243	4.302	vs
(400)	27.95	27.65	3.193	3.227	m
(430)	34.23	34.77	2.619	2.580	w
(011)	11.56	11.77	7.656	7.520	m
($\bar{1}$11)	14.53	14.73	6.097	6.014	m
(121)	19.59	19.78	4.532	4.490	m
($\bar{2}$21)	26.72	26.95	3.337	3.308	s
(431)	34.96	35.53	2.566	2.527	w
(002)	14.22	14.16	6.226	6.256	s
(302)	25.19	25.12	3.536	3.545	m
($\bar{2}$22)	29.64	29.71	3.014	3.007	w
(402)	31.66	31.19	2.826	2.868	w
(432)	37.74	37.72	2.384	2.385	w
(003)	21.21	21.30	4.189	4.170	vw
(013)	22.99	23.33	3.868	3.813	m
(123)	27.83	28.33	3.206	3.150	w
($\bar{1}$23)	30.48	30.52	2.933	2.929	w
($\bar{2}$23)	33.75	33.84	2.656	2.649	m
(004)	28.77	28.54	3.103	3.128	s
(224)	34.99	35.41	2.564	2.535	m
($\bar{2}$24)	38.76	38.77	2.323	2.311	m
(025)	40.87	40.85	2.208	2.209	w

[a] The calculated data listed are based on a monoclinic II unit cell with a = 13.30 Å, b = 9.693 Å, c = 12.51 Å, and γ = 76.1°. [b] The intensities are semiquantitatively estimated via a microdensitometer. The intensities are classified as very strong (vs), strong (s), medium (m), weak (w), and very weak (vw).

Figure 4 shows the X-ray fiber diagram of the crystal diffraction photograph for the as-spun (quenched) TPA/PHQ/PEHQ copolyester. Following the same procedure, one can determine the crystal unit cell of the quenched form, which is a monoclinic I: a = 13.04 (±0.02) Å, b = 9.514 (±0.01) Å, c = 12.24 (±0.02) Å, and γ = 80.8° (±0.1°). This leads to a unit cell volume of 1499.3 Å^3. The calculated crystallographic density is thus 1.464 g/cm^3. The experimental density is 1.371 g/cm^3. Detailed 2θ and d spacing data (calculated and observed) are listed in Table II.

The DSC heating traces of both quenched and annealed fibers with free ends show only one main transition peak at 605 and 619 K with heats of transition of 2.47 and 3.31 kJ/mol, respectively.

Isothermal Kinetic Studies. We have observed that in this copolyester two transition processes exist (see below). The temperature range of this isothermal kinetic study for the fast transition process was limited to 590–600 K due to the nature of the transition. The temper-

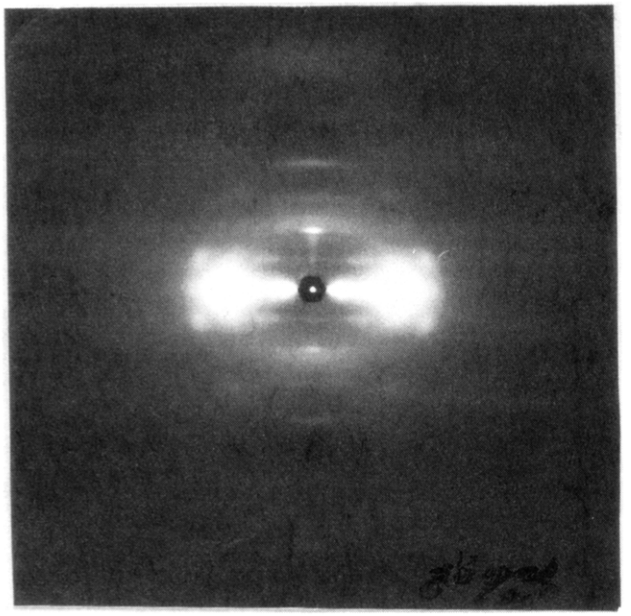

Figure 4. Wide-angle X-ray diffraction photograph of the as-spun TPA/PHQ/PEHQ copolyester fibers (quenched).

Table II
Experimental and Calculated Crystallographic Parameters of the Monoclinic I Crystal Unit Cell for Quenched TPA/PHQ/PEHQ As-Spun Fibers[a]

	2θ, deg		d spacing, Å		
(hkl)	exptl	calcd	exptl	calcd	intensity[b]
(100)	6.879	6.863	12.85	12.88	vs
(200)	13.77	13.76	6.431	6.437	m
(2̄10)	17.94	17.90	4.944	4.956	s
(300)	20.77	20.70	4.277	4.292	s
(400)	27.65	27.71	3.226	3.219	w
(011)	11.84	11.88	7.474	7.452	w
(1̄11)	14.61	14.46	6.063	6.124	w
(1̄21)	20.25	20.40	4.385	4.352	w
(321)	26.81	26.83	3.325	3.323	m
(002)	14.40	14.47	6.151	6.120	m
(102)	16.15	16.03	5.488	5.527	w
(302)	25.40	25.35	3.507	3.514	w
(003)	22.00	21.78	4.040	4.080	m
(103)	22.75	22.86	3.909	3.889	w
(004)	29.06	29.18	3.073	3.060	m

[a] The calculated date listed are based on a monoclinic I unit cell with $a = 13.04$ Å, $b = 9.514$ Å, $c = 12.24$ Å, and $\gamma = 80.8°$. [b] The intensities are semiquantitatively estimated via a microdensitometer. The intensities are classified as very strong (vs), strong (s), medium (m), weak (w), and very weak (vw).

ature range of the study for the slow transition process was between 520 and 580 K. Please note that an exothermic peak can be observed at 576 K when the nonisothermal experiment was carried out at a −10 K/min cooling rate.

Figure 5 shows, as an example, the relationships between heats of transition (ΔH_d) and logarithimic times (log t_c) for the fast transition process at three different temperatures. One can find that, indeed, the time to reach the maximum ΔH_d here is very short. After about 5 min, at $T_c = 596$ K, for example, this transition process has been completed. Applying the Avrami treatment leads to a straight line between log [−ln (1 − $\Delta H_d/\Delta H_d$*)] and log t_c in the initial transition stage, where ΔH_d* is the maximum of the heat of transition (we adopted ΔH_d* = 2.5 kJ/mol), as shown in Figure 6 at these temperatures. Of special interest is that the values of the initial slopes of the straight lines are close to 2, as shown in this figure.

For the slow transition process, Figure 7 represents a

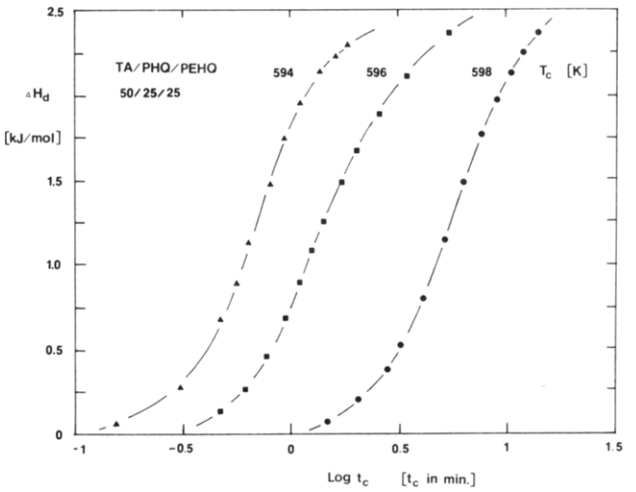

Figure 5. Relationship between the heat of transition (ΔH_d) and logarithmic time (log t_c) for the fast transition process at three different isothermal temperatures.

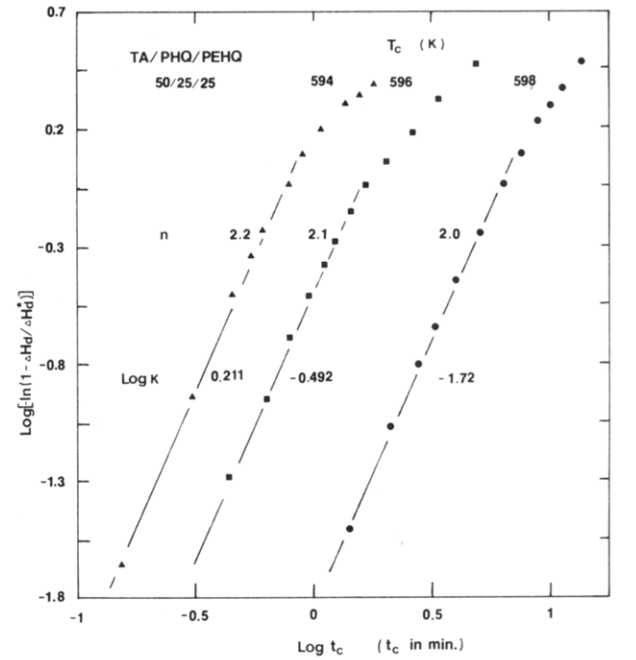

Figure 6. Avrami treatments of the kinetics for the fast transition process at three different isothermal temperatures.

set of DSC heating traces after the samples were kept at $T_c = 550$ K for different times (t_c). At short t_c it is clear that only a peak contributed by the fast transition process can be observed at a transition temperature of T_d(h) ≅ 605 K, with a very small shoulder in the low-temperature range. With increasing t_c, this shoulder gradually develops to become a second peak on the low-temperature side of the first peak. This peak temperature and its heat of transition increase with t_c. Figures 8 and 9 illustrate for transition processes the relationships between ΔH_d and log t_c and between T_d and log t_c at different T_c, respectively. It is evident that with increasing T_c, the ΔH_d of the slow transition process increases and that of the fast transition process decreases from 2.08 kJ/mol at $T_c = 530$ K to 1.02 kJ/mol at $T_c = 580$ K. However, at each T_c, the ΔH_d of the fast transition process remains almost constant. The transition temperature, T_d[l], increases linearly with logarithmic time, log t_c, at each T_c for the slow transition process, so does that of the fast transition process, [T_d(h)], but in a much gentler manner.

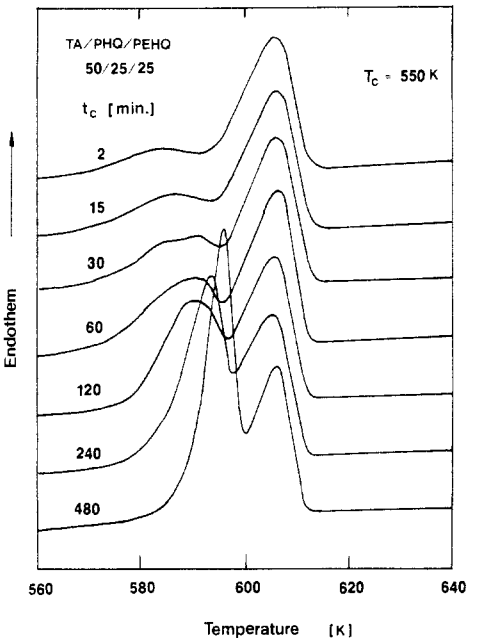

Figure 7. Set of DSC heating traces for the TPA/PHQ/PEHQ copolyester after isothermal crystallization at T_c = 550 K for different times, t_c.

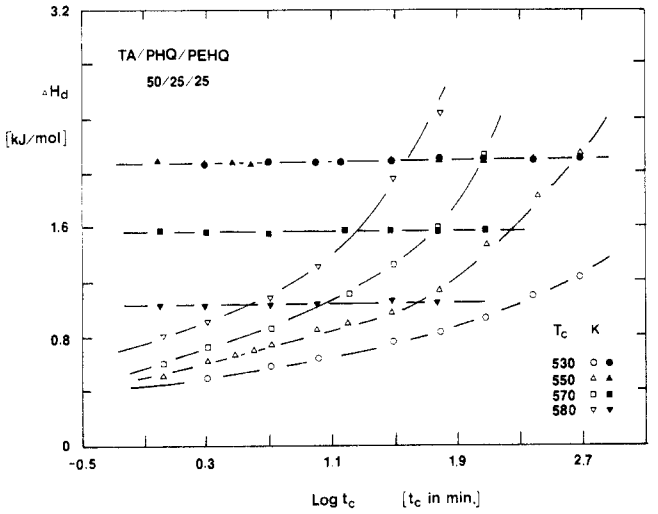

Figure 8. Relationship between the heat of transition (ΔH_d) and logarithmic time (log t_c) for the two transition processes at different isothermal temperatures. The filled symbols represent the fast transition processes, and the open symbols represent the slow transition processes: T_c = 530 (○, ●), 550 (△, ▲), 570 (□, ■) and 580 K (▽, ▼).

Figure 10 shows the Avrami treatment for the kinetics of the slow transition process (assuming that ΔH_d^* = 5.0 kJ/mol). One can find that this transition is characterized by a very low Avarami exponent, n, in the range 0.15–0.38, which increases slightly with T_c.

Discussion

The TPA/PHQ/PEHQ copolyester provides an opportunity to take a close look at the lowering of the transition temperature in this copolyester, namely, a path of disturbing the lateral packing of the crystals. As we observed, for this copolyester, two transition processes can be identified. However, a simple extension of the explanation we addressed in ref 2 may lead to confusion.

First of all, the two transition processes observed here do not correspond to two different crystal packings as in the cases of Vectra and Xydar copolyesters,[2] but instead,

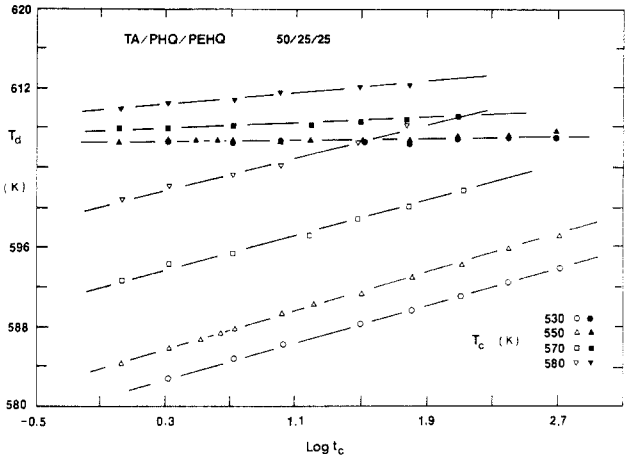

Figure 9. Relationship between the transition temperature (ΔT_d) and logarithmic time (log t_c) for the two transition processes at different isothermal temperatures. The filled symbols represent the fast transition processes, and the open symbols represent the slow transition processes: T_c = 530 (○, ●), 550 (△, ▲), 570 (□, ■), and 580 K (▽, ▼).

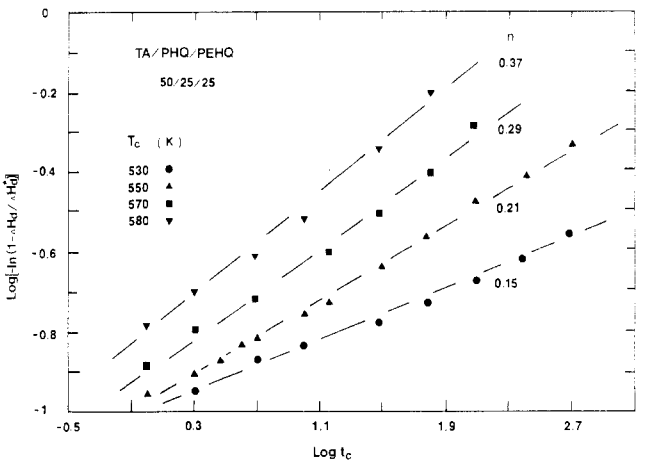

Figure 10. Avrami treatment of the kinetics for the slow transition process at different isothermal temperatures.

the crystals grown in these two processes are both monoclinic, having different unit cell sizes and angles (γ). It is quite evident that with the large pendant side groups, cylindrical symmetry of the molecules along their chain directions no longer exists. As a result, the possibility of hexagonal packing in the quenched form of this copolyester should be ruled out.

The second question that should be raised is regarding the monoclinic packing determination. Recently, Hong and Blackwell have reported monoclinic (with γ = 90°) (or orthorhombic) packings in two copolyesters with very similar chemical structures,[8,9] which is slightly different from our analyses. Using our refinement program, recalculation of the observed d spacing of Hong and Blackwell leads to a fit to an orthorhombic structure rather than a monoclinic one (the standard deviation of the monoclinic structure is about five times higher than that of the orthorhombic one). On the other hand, our observed d spacing data can only fit to a monoclinic structure. The deviation of this fit is about 50% smaller than the fit of Hong and Blackwell's data for the orthorhombic structure, but it is still within 1 order of magnitude. Such difference between Hong and Blackwell's results[8,9] and ours might be caused by different (even slight) randomness in the chemical structures, polymerization procedures, and/or annealing conditions.

It is of further interest to see the difference between the unit cell sizes of the fibers in their as-spun (quenched) form and those of the fibers in their annealed form. In general, an annealing process leads to a decrease of the unit cell volume and, correspondingly, an increase of crystallographic density, such as in the cases of polyethylene,[10] polypropylene,[11] and poly(ethylene terephthalate).[12] Nevertheless, in our case of the TPA/PHQ/PEHQ copolyester, the unit cell volume of the annealed fibers increases by expanding the b axis from 9.514 to 9.693 Å, the a axis from 13.04 to 13.30 Å, and the c axis from 12.24 to 12.51 Å. A similar situation has been reported in the case of poly(p-phenyleneterephthalamide) (PPTA) fibers.[13,14] After annealing at 873.2 K for a very short period of time (a few seconds), the a axis of the PPTA unit cell (monoclinic packing with $\gamma = 90°$) expands from 7.80 Å in its as-spun form to 9.39 Å. At the same time, the b axis expands from 5.18 to 5.20 Å and the c axis from 12.9 to 13.0 Å, respectively.

A qualitative explanation of such an expansion after annealing in our case can be attempted. In order to closely fit the large pendant side groups in a three-dimensional space, the chain conformation along the c axis has to be slightly twisted when the fibers are in the as-spun form (quenched). After annealing at high temperature under load, such a conformation becomes more extended (c-axis expansion). As a result, the pendant side groups no longer keep the close packing with their neighboring chains as in the as-spun form, which is caused by a slight twisting of the backbone chains. The steric hindrance of the pendant side groups with their neighboring chains may cause the expansions along the a and b axes. The experimental density measurements of those fibers in both as-spun and annealed forms are a clear indication of such expansion. Although the heat of transition in the annealed form is about 33% higher than that in the as-spun form, the former experimental density is still about 1% lower than that in the latter case.

Third, when one discusses the transition temperatures of the two processes in this copolyester, the same trend as reported in refs 1 and 2 can be found; namely, the fast transition process shows a higher transition temperature and the slow transition process a lower transition temperature. One has to ask, again, what is the cause of this phenomenon? In this case, the first possible explanation can be from thermodynamic considerations. In this copolyester, the entropy change during the transition of the fast process should not be too much different from that of the slow process, since the hexagonal packing is forbidden. However, a relatively large difference of the enthalpy changes between the two transition processes can be expected due to an expansion of unit volume (6% increase from the as-spun to the annealed fibers). On the basis of the thermodynamic equation $T_d = \Delta H_d/\Delta S_d$, the transition temperature T_d of the slow process is generally lower than that of the fast process, mainly because of a relative smaller contribution of ΔH_d in the slow transition process. The second possible explanation can be based on kinetic effects. The fast transition process may occur in relatively ordered domains. Also, for the slow transition process, if the size of the annealed crystals is large enough and the crystal is perfect enough, we may push its transition temperature higher and close to the T_d of the fast transition process as shown in Figure 8.

Finally, it has been shown that for oriented rigid macromolecules growing longitudinally, the Avrami treatment can be satisfied as two-dimensional growth if the molecules are parallel. The Avrami exponent (n) must thus be 2 in the case of predetermined nuclei.[1] Our transition kinetics of the fast process indicate just such a kind of crystal growth with $n \simeq 2$. Consequently, the transition kinetics can be recognized as a type of nucleation-controlled growth, which is different from the solidification shown by the fast transition process of Vectra and Xydar copolyesters. It is evident that the latter is basically a mesophase transition from their nematic to conformationally disordered (condis) phases,[1,2,15] and the former is a nematic to crystalline phase transition. One can also find that the kinetics of the fast transition process in this TPA/PHQ/PEHQ copolyester is not as fast as those in Vectra and Xydar copolyesters. On the other hand, the transition kinetics of the slow process in this copolyester shows low Avrami exponents, which may arise due to nonnegligible fractions of crystal nuclei or change of growth rate during crystallization in addition to low dimensional growth.[16]

The independence of the growth from these two transition processes is quite evident, because the monoclinic packing formed during the fast process has different unit cell sizes and angles (γ), and therefore, it cannot act as nuclei to stimulate the crystal growth of the slow transition process. The consistency of the heat of transition with respect to time for the fast process reveals that in the monoclinic packing, molecular motions are largely hampered. The large pendant side groups should be a major factor in hindering such motions. Furthermore, of special interest is that the heat of transition formed during the fast transition process decreases with increasing T_c above 550 K, indicating clearly that the kinetics of the fast transition process slow down at high T_c. On the other hand, the kinetics of the slow transition process speed up with increasing T_c. As a result, the crystal development of the fast transition process is interrupted by the crystal growth of the slow process. One can see that, in fact, when T_c is below 550 K the fast transition process can be fully developed. This also demonstrates the limitation of molecular motion in the TPA/PHQ/PEHQ copolyester. Nevertheless, detailed experimental observations of molecular motion in the solid state are necessary before we can discuss this further.

Conclusions

(1) In the TPA/PHQ/PEHQ copolyester studied, two transition processes are identified: the fast process forming a crystal with a monoclinic I packing of $a = 13.04$ Å, $b = 9.514$ Å, $c = 12.24$ Å, and $\gamma = 80.8°$ and the slow process forming a crystal with a monoclinic II packing of $a = 13.30$ Å, $b = 9.693$ Å, $c = 12.51$ Å, and $\gamma = 76.1°$.

(2) Both transition processes are basically crystallization processes from the nematic state; no condis form is involved. The fast process shows a higher transition temperature since the change of enthalpy between its nematic melt and monoclinic I crystal is larger than that of the slow process due to a smaller unit cell size in the as-spun (quenched) form.

(3) The kinetic relationship between these two transition processes indicates that both crystal growths are independent. Furthermore, the development of the slow process is hampered by the previously grown crystals in the fast process.

(4) In this copolyester, the crystallization process in the fast transition process is nucleation controlled, and the crystallization can be interrupted by the crystal growth of the slow transition process at high T_c (above 550 K).

Acknowledgment. This work was partially supported by the Research Challenge Grant of Ohio State Regent through the University of Akron.

References and Notes

(1) Cheng, S. Z. D. *Macromolecules* **1988**, *21*, 2475.
(2) Cheng, S. Z. D.; Janimak, J. J.; Zhang, A.-Q.; Zhou, Z.-L. *Macromolecules* **1989**, *22*, 4240.
(3) Biswas, A.; Blackwell, J. *Macromolecules* **1988**, *21*, 3146, 3152, 3158.
(4) Field, N. D.; Baldwin, R.; Layton, R.; Frayer, P.; Scardiglia, F. *Macromolecules* **1988**, *21*, 2155.
(5) Blackwell, J.; Cheng, H.-M.; Biswas, A. *Macromolecules* **1988**, *21*, 39.
(6) Chivers, R. A.; Blackwell, J.; Gutierrez, G. A.; Stamatoff, J. B.; Yoon, H. In *Polymeric Liquid Crystals*; Blumstein, A., Ed.; Plenum: New York, 1985; p 153.
(7) Blackwell, J.; Gutierrez, G. A.; Chivers, R. A. In *Polymeric Liquid Crystals*; Blumstein, A., Ed.; Plenum: New York, 1985; p 167.
(8) Hong, S. K.; Blackwell, J. *Polymer* **1989**, *30*, 225.
(9) Hong, S. K.; Blackwell, J. *Polymer* **1989**, *30*, 780.
(10) Zhang, A.; Chen, K.; Lu, P.; Wu, Z.; Qian, B. *Bull. Am. Phys. Soc.* **1988**, *33*, 504.
(11) Hikosaka, M.; Seto, T. *Repr. Progr. Polym. Phys. Jpn.* **1969**, *12*, 153.
(12) Sun, T.; Zhang, A.-Q.; Li, F.; Porter, R. S. *Polymer* **1988**, *29*, 2115.
(13) Northolt, M. G. *Eur. Polym. J.* **1974**, *10*, 799. See also: Northolt, M. G.; van Aartsen, J. J. *J. Polym. Sci., Part B* **1973**, *11*, 333.
(14) Yabuki, K.; Ito, H.; Ota, T. *S. Gakkaishi* **1975**, *31*, 524; **1976**, *32*, 55.
(15) Wunderlich, B.; Moller, M.; Grebowicz, J.; Baur, H. *Adv. Polym. Sci.* **1988**, *87*, 1.
(16) Cheng, S. Z. D.; Wunderlich, B. *Macromolecules* **1988**, *21*, 3327.

Evaluation of Nonradiative Energy Transfer as a Means of Probing Polymer Miscibility and Polymer Phase Separation

M. Henrioulle-Granville,[1] K. Kyuda,[2] R. Jérôme,* and Ph. Teyssié

Laboratory of Macromolecular Chemistry and Organic Catalysis, University of Liège, Sart-Tilman, 4000 Liège, Belgium

F. C. De Schryver

Laboratory of Molecular Dynamics and Spectroscopy, KU Leuven, Department of Chemistry, Celestijnenlaan 200F, B-3030 Heverlee, Belgium. *Received January 31, 1989; Revised Manuscript Received July 17, 1989*

ABSTRACT: The ability of nonradiative energy transfer (NRET) to probe polymer miscibility and polymer phase separation is discussed for blends of PVC and PMMA of various tacticity. The sensitivity of that fluorescence technique depends on the range between the lower (total miscibility) and the upper value (complete immiscibility) of the ratio of the intensity emitted by naphthalene and anthracene (I_N/I_A) used to label PVC and PMMA, respectively. Although measurements of the lower limit are reproducible, determination of the upper limit is quite a problem, making uncertain the analysis of any system phase separated on a scale of at least 2–3 nm. At and above this dimension, solvent-cast PVC/PMMA blends appear to be completely miscible whatever the PMMA tacticity. That the I_N/I_A ratio of the PVC/PMMA blends changes with the tacticity of PMMA is interpreted as an effect of chain conformation on the probability of intermolecular interactions. For instance, the more rigid the PMMA is in relation to its tacticity, the more extended the intermolecular contacts with PVC seem to be. Finally, heating a monophase PVC/PMMA blend above the LCST does not lead to an increase in the I_N/I_A ratio great enough to detect phase separation.

Introduction

Most polymers are immiscible and form multiphase blends when mixed together.[3] A number of methods have been proposed to probe polymer blends and to determine whether they are homogeneous (monophase) or not.[4] Optical clarity is the simplest test, which is only convenient when both the difference in the refractive index of the mixed polymers is large enough and the information is at a scale larger than 100 nm. The most commonly used techniques to measure the glass transition are differential scanning calorimetry, dynamic mechanical testing, and microscopy (optical or electron depending on the miscibility level). Since the resolution power of all these techniques is different, a given blend might be declared miscible by using one method (i.e., T_g measurements) and immiscible according to a higher resolution technique (i.e., electron microscopy).

Today a great deal of attention is paid to novel techniques able to probe multicomponent system at a scale of a few nanometers, for example, solid-state NMR[5,6] and fluorescence techniques such as excimer fluorescence, fluorescence microscopy, and nonradiative energy transfer. Frank et al.[7] have used excimer fluorescence to characterize the miscibility of poly(2-vinylnaphthalene) with poly(methyl methacrylate) and polystyrene. Poly(2-vinylnaphthalene) (guest) comprises excimer-forming chromophores as constitutive pendant groups and has been mixed with a large percentage of the second partner (host). Using fluorescence microscopy, Monnerie et al.[8] have determined the boundaries (binodal and spinodal curves) of the phase diagram of anthracene-labeled polystyrene/poly(vinyl methyl ether). Finally, Morawetz et al.[9] and later on Teyssié et al.[10] have used nonradiative energy transfer (NRET) to estimate the degree of miscibility of several polymer pairs.

The main purpose of this study is a critical analysis of

0024-9297/90/2223-1202$02.50/0